Electrophoresis of active Janus particles

P. Bayati [ID], and A. Najafi [ID]

View Online   Export Citation   CrossMark

Electrophoresis of active Janus particles

P. Bayati[1,a] (ID) and A. Najafi[1,2] (ID)

AFFILIATIONS

[1] Department of Physics, Institute for Advanced Studies in Basic Sciences (IASBS), Zanjan 45137-66731, Iran
[2] Research Center for Basic Sciences & Modern Technologies (RBST), Institute for Advanced Studies in Basic Sciences, Zanjan, Iran

[a] **Present address:** LPTMS, UMR 8626, CNRS, Univ. Paris-Sud, Université Paris-Saclay, 91405 Orsay, France.
E-mail: parvin.bayati@u-psud.fr.

ABSTRACT

We theoretically consider the dynamics of a self-propelled active Janus motor moving in an external electric field. The external field can manipulate the route of a Janus particle and force it to move toward the desired targets. To investigate the trajectory of this active motor, we use a perturbative scheme. At the leading orders of surface activity of the Janus particle and also the external field, the orientational dynamics of the Janus particles behave like a mathematical pendulum with an angular velocity that is sensitive to both the electric field and surface activity of the motor.

Published under license by AIP Publishing. https://doi.org/10.1063/1.5101023

I. INTRODUCTION

Among all microswimmers,[1–3] active Janus particles are novel and one of the most interesting micromotors with many promising and realized applications.[4,5] Since its first realization,[6] many applications of active Janus particles have been achieved successfully, including effective and intelligent cargo[7–12] and drug delivery,[13–18] the ability to enter into living cells,[19–22] detecting and healing microdefects in microchips,[23,24] and nanopatterning techniques.[25] Also, it has been shown that these motors are able to clean water of organic or inorganic pollutants such as bacteria and heavy metal compounds more effectively.[26–34] Designing chemical and biosensors is another progress in the application of active Janus particles.[18,35,36]

Like the first synthesized models,[6,37–39] active Janus motors usually are made in the form of micron-sized rods or spheres consisting of two parts with distinct surface chemical properties. These motors operate by setting up decomposition of chemical molecules in the fluid and converting chemical energy into mechanical work, often in the form of a directed or rotational motion.[40–44] Besides substantial efforts devoted to understanding the mechanism involved in the motion of a single motor,[45–56] studying their dynamics in complex environments, such as geometrical confinements and obstacles, crowded environments with high densities of active or passive particles, and non-Newtonian media, is also of great interest in order

to control their behavior in various applications.[57–72] In most of the applications, having the ability to precisely align and guide Janus motors in predefined directions toward targets is a crucial experimental need.[10,11,73] Modulating the velocity of self-phoretic Janus motors by applying a gradient to the concentration of involved chemical molecules is examined experimentally.[7,9,11] In some biological applications, a ferromagnetic core, such as nickel, has been attached to Janus motors so that torque from an external magnetic field can change the direction.[7–10] Optical and chemical gradients,[74–76] activation field gradients,[77,78] and acoustic tweezers[79] are some other ways to guide active Janus particles.

Electrical properties of most catalytic micromotors[6,42,50] suggest that an electric field can be an alternative or even better candidate to control the motion of self-phoretic particles. Moreover, pickup and release of cargos through induced dipolar interactions between a Janus motor and the cargos can be achieved more easily by applying an electric field rather than other tools.[11,73] In this regard, the electrophoresis of catalytic Janus particles has been investigated experimentally in Ref. 68 (see Fig. 3). A spherical polystyrene colloidal particle with a platinum cap immersed in the solution of H_2O_2 has been considered. Driven by self-phoresis, the particle moves toward the polystyrene side. Their observations show that applying an electric field causes the particle to rotate and realign its direction of symmetry parallel to the field. Therefore, the particle moves in the direction of the electric field.

Here, we theoretically investigate the dynamics of an active Janus particle in the presence of a uniform external electric field. The particle is a nonconducting spherical colloid with active chemical sites that are distributed asymmetrically over it. This active particle is immersed in an electrolyte solution. As a result of chemical reactions, a gradient of cations and anions will be developed in the media and this eventually provides the self-propulsion force necessary to operate the motor.[80] Furthermore, an external electric field is also applied to this system.

The electric field acted on a passive charged particle causes the well known phenomena of electrophoresis.[81,82] For active colloids, in addition to the electrophoresis, the external electric field will affect the dynamics of the Janus particle by modifying and deforming the electrostatic potential and Debye layer around that particle. We will show that this effect has a main role in the dynamics of the active Janus particle by imposing an aligning torque on the particle.

The organization of this paper is as follows: in Sec. II, we introduce the model of the active Janus motor. Sections III and IV are devoted to outlining the main equations governing the motion of the motor and introduce the approximations to simplify the equations. We proceed by providing a perturbation expansion and obtaining analytical results in Sec. V. Finally, the results and discussions are presented in Sec. VI.

II. MODEL SYSTEM

As shown in Fig. 1, consider a spherical active particle with radius a immersed in a bulk electrolyte solution with electric permeability ε_r and hydrodynamic viscosity η. For simplicity, we consider the case of a symmetric 1:1 electrolyte, i.e., the valencies of two ionic species, cations and anions, are $Z_\pm = \pm 1$, respectively. We denote the bulk number density of each ionic species by $n_+^b = n_-^b := n_\infty$ and their diffusion constants as D. The particle is charged, and the electrostatic potential on the surface of the particle, relative to the potential in the bulk solution, is denoted by ψ_s. As demonstrated in Fig. 1, the surface of the particle consists of two parts with distinct chemical activity.[80] The activity of the surface of the particle triggers a set of chemical reactions asymmetrically; both ionic species are released ("emitted") simultaneously on the north hemisphere of the particle with rate $\dot{Q}$. On the other hand, both cations and anions are reduced ("annihilated") on the south hemisphere by the same rate given at the emitting part. Physically, this can be realized, e.g., by breaking up neutral molecules ("fuel") present in the solution on the emitting side that drives the whole system out of chemical equilibrium. Then, on the other side of the particle, reactions start to recombine the extra ions with neutral molecules in order to bring back the system to chemical equilibrium with a conserved number of molecules. Moreover, the particle is assumed to be nonconductive; therefore, the chemical reactions on its surface do not have any electrical effect on the particle, i.e., releasing/annihilating of ions does not change the uniform surface charge of the particle. Such a Janus motor is often made of an insulator, e.g., silica or polystyrene, with a thin layer of a catalyst coated on some parts of the particle.[44] The physical behavior of other types of active Janus motors, such as light-activated Janus particles moving in binary mixtures,[39] has some similarities to the model described here.

In addition to the model described above, other similar theoretical models for an active Janus particle are possible which share the same concept of releasing/annihilating ions (or other types of solute particles) to create phoretic forces.[45,83] However, the distribution of reactions recombining extra ions or solute molecules differs in these models. Since all of these models share the same physics, and especially leads to similar results for an isolated Janus particle,[84] in this study, we focus only on the simple model explained above.

Following the chemical processes, local changes in the density of ions around the particle will develop and subsequently drive the system out of mechanical equilibrium. For such an isolated active Janus motor and in the absence of the external field, we denote the self-propulsion active velocity by $\mathbf{U}^a$. From the other hand and for a passive Janus particle with a constant and symmetric surface potential, moving in an external electric field, the phenomenon of electrophoresis exerts a force to the particle. We denote this electrophoretic velocity with $\mathbf{U}^e$. Here, we would like to consider both mechanisms of activity and electrophoresis, simultaneously. Decomposing the active and electrophoresis parts in the velocities as

$$\mathbf{U} = \mathbf{U}^a + \mathbf{U}^e + \mathbf{U}^{ae}, \quad \boldsymbol{\Omega} = \boldsymbol{\Omega}^{ae}, \qquad (1)$$

we aim to calculate the contributions to the linear and angular velocities denoted by $\mathbf{U}^{ae}$ and $\boldsymbol{\Omega}^{ae}$ that are functions of the interplay between activity and electrophoresis. Promised by symmetry principles, neither activity nor electrophoresis is able to solely apply torque on the particle and enforce it to rotate. This is reflected in the above equation for the angular velocity where contributions from activity or electrophoresis are not considered. Furthermore, we will see in Sec. V that the above form of decomposition will help us in developing some approximating procedures to deal with the complicated mathematics of this problem.

FIG. 1. Illustration of a spherical and chemically active particle in a uniform electric field $\mathbf{E} = E\,\hat{\epsilon}$. The surface of the particle consists of two hemispheres with distinct chemical activity. Chemical reactions release both positive and negative ions (blue and red dots) on the north hemisphere (depicted in yellow) and annihilate them on the south hemisphere (depicted in gray). The unit vectors $\hat{\mathbf{t}}$ and $\hat{\epsilon}$ indicate the symmetry axis of the active particle and the direction of the electric field, respectively. Self-propulsion and the electrophoresis of the particle allow it to move with translational and rotational velocities denoted by $\mathbf{U}$ and $\boldsymbol{\Omega}$, respectively.

In the following, we proceed with giving the main equations governing the dynamics of the motor. Then, by introducing some simplifications, we will get a set of equations that can be solved analytically.

III. GOVERNING EQUATIONS

Fluid velocity $\mathbf{u}(\mathbf{r})$, pressure $p(\mathbf{r})$, electric potential $\psi(\mathbf{r})$, and ionic densities $n_{\pm}(\mathbf{r})$ are main fields in our problem that need to be determined. Before writing the dynamical equations, it is convenient to define a dimensionless system of units. We use the radius of the Janus particle a, thermal potential $\psi_0 = (k_B T/e)$, bulk density of ions n_∞, and a characteristic velocity given by $v_0 = (k_B T/e)^2 (\varepsilon_r/\eta a)$ to make all quantities nondimensional, where k_B is the Boltzmann constant, T is the temperature, and ρ and η are the fluid density and viscosity, respectively. In this dimensionless system, the hydrodynamics of the incompressible Newtonian fluid is governed by the following Stokes and continuity equations:

$$\nabla^2 \mathbf{u}(\mathbf{r}) - \nabla p(\mathbf{r}) + \nabla^2 \psi(\mathbf{r}) \nabla \psi(\mathbf{r}) = 0, \quad \nabla \cdot \mathbf{u}(\mathbf{r}) = 0. \quad (2)$$

One should note that in writing the above equations, we have assumed that the Reynolds number defined as $\mathrm{Re} = (\rho U a/\eta)$ is very small for microscales where U is the characteristic velocity of the motor. The electrostatic interactions of ions with the local potential $\psi(\mathbf{r})$ lead to a distribution of body forces in the fluids given by $\nabla^2 \psi(\mathbf{r}) \nabla \psi(\mathbf{r})$. The electrostatic potential obeys the Poisson equation,

$$\delta^2 \nabla^2 \psi = -\frac{1}{2}(n_+ - n_-), \quad (3)$$

where $\delta = 1/(\kappa a)$ with $1/\kappa = \sqrt{\varepsilon_r k_B T/2e^2 n_\infty}$ gives the dimensionless thickness of the "Debye layer." This Debye layer measures the the equilibrium thickness of the fluid around a colloidal particle where counter ions are accumulated there and screen the charge of colloid.[81,82] The distribution of the ionic species is governed by the continuity equation for the corresponding number densities,

$$\frac{\partial n_{\pm}(\mathbf{r})}{\partial t} + \nabla \cdot \mathbf{j}_{\pm}(\mathbf{r}) = 0. \quad (4)$$

The ionic currents $\mathbf{j}_{\pm}(\mathbf{r})$ are given by the phenomenological expressions as

$$\mathbf{j}_{\pm}(\mathbf{r}) = -\nabla n_{\pm}(\mathbf{r}) \mp n_{\pm}(\mathbf{r}) \nabla \psi(\mathbf{r}) + \mathcal{P}e \, n_{\pm}(\mathbf{r}) \mathbf{u}(\mathbf{r}). \quad (5)$$

The first two terms on the right hand side of the above equation represent the transport by diffusion of ions and drift due to the electric force, respectively. The third term is the convection due to the flow of fluid. Here, Péclet is a dimensionless number that describes the ratio of the transport via convection by the flow to the thermal diffusion and it is given by $\mathcal{P}e = (a v_0/D)$.

Equations (2)–(4) must be solved subject to appropriate boundary conditions at the surface of the motor and at infinity. We start with the boundary conditions at the surface of the motor. The chemical activity on the surface of the Janus motor is given by the following condition on the ionic fluxes:

$$\hat{\mathbf{n}} \cdot \mathbf{j}_{\pm}(\mathbf{r} = \hat{\mathbf{n}}) = \dot{q} \, \hat{\mathbf{t}} \cdot \hat{\mathbf{n}}, \quad (6)$$

where $\dot{q} = \dot{Q}a/D$ is a dimensionless number defining the strength of surface activity of the Janus particle. The unit vector locally normal to the surface of the motor is denoted by $\hat{\mathbf{n}}$, and the angular configuration of the Janus particle is denoted by a unit vector denoted by $\hat{\mathbf{t}}$. The electrostatic potential and the fluid velocity in a comoving frame should satisfy the following boundary condition at the surface of the motor:

$$\mathbf{u}(\mathbf{r}) = 0, \quad \psi(\mathbf{r}) = \psi_s, \quad \mathbf{r} = \hat{\mathbf{n}}. \quad (7)$$

At infinity, the boundary conditions read

$$\mathbf{u}(\mathbf{r}) = -\mathbf{U} - \mathbf{\Omega} \times \mathbf{r}, \quad \nabla \psi(\mathbf{r}) = -\epsilon \, \hat{\epsilon}, \quad n_{\pm} = 1, \quad r \to \infty, \quad (8)$$

where $\epsilon = E \, ea/(k_B T)$ is a dimensionless number characterizing the strength of the external electric field and $\hat{\epsilon}$ is a unit vector showing its direction. $\mathbf{U}$ and $\mathbf{\Omega}$ are the translational and angular velocities of the motor, respectively. The motor experiences hydrodynamic and electrostatic forces and torques that are given by the Stokes hydrodynamic and Maxwell electrostatic stress tensors. Considering the fact that the motion of a microscale Janus particle takes place at low Reynolds condition, net force and torque should vanish,

$$\mathbf{F} = \oint_S \left\{ -p\mathbb{I} + \nabla\mathbf{u} + (\nabla\mathbf{u})^T + \nabla\psi\nabla\psi - \frac{1}{2}\nabla\psi \cdot \nabla\psi\mathbb{I} \right\} \cdot \hat{\mathbf{n}} \, dS = 0, \quad (9)$$

$$\boldsymbol{\tau} = \oint_S \mathbf{r} \times \left\{ -p\mathbb{I} + \nabla\mathbf{u} + (\nabla\mathbf{u})^T + \nabla\psi\nabla\psi - \frac{1}{2}\nabla\psi \cdot \nabla\psi\mathbb{I} \right\} \cdot \hat{\mathbf{n}} \, dS = 0. \quad (10)$$

Here, $\mathbb{I}$ stands for the unit matrix and superscript T denotes the matrix transposition.

IV. APPROXIMATIONS

Before solving the equations, it is instructive to consider the order of magnitude for relevant physical parameters in a typical system. We will see that realistic values of parameters will allow us to introduce a couple of approximations that can simplify the mathematical equations we have presented in Sec. III. A micromotor with $a \sim 1 \, \mu$m moves with a velocity about $1 \, \mu$m s^{-1} in an aqueous solution with viscosity $\eta \sim 10^{-3}$ Pa s.[6,37] Furthermore, in an electrolyte solution, such as 0.001M solution of KCL at room temperature, the diffusion and the bulk density of ions are of order $D \sim 10^{-9}$ m^2 s^{-1} and $n_\infty \sim 10^{23}$ m^{-3}, respectively.[82] So, we can see that $\delta \sim 10^{-3}$ and $\mathcal{P}e \sim 10^{-1}$. Consequently, we can make great simplifications in dynamical equations by considering the conditions of $\mathcal{P}e \ll 1$ and $\delta \ll 1$ to obtain approximate equations. For further simplification of the model, we assume that the kinetics of the decomposition/reduction is in the "reaction limited" regime with $\dot{q} = \dot{Q}a/Dn_\infty \ll 1$,[85] i.e., diffusion of ions is much faster than emission/annihilation of ions.

The main simplification is related to the concept of the Debye layer. For most experimentally realizable systems, as noted above, the thickness of the Debye layer is much smaller than the size of the particle, i.e., $\delta = 1/\kappa a \ll 1$. At this condition, we use a macroscale description developed by Yariv and co-workers[86–88] and divide the

fluid domain into two regions: "inner" (within the Debye layer) and "outer" (outside the Debye layer) parts. In this macroscale description, the goal is to obtain effective macroscale properties of the nearly electro-neutral outer region. In the following, we will see that the effective physical properties at the bulk can be achieved by applying proper boundary conditions on the outer surface of the Debye layer on macroscale fields.

The equations governing the dynamics can be solved for each regions separately and finally matched to the solutions on the edge of the double layer.[80,86,87,89] The velocity of the Janus particle, $\mathbf{U}$, which we would like to evaluate, appears in the outer region problem as a boundary condition at infinity (in the comoving frame).

In the inner region, because of a very thin film of fluid, the surface of the motor can be approximated as a planar wall. The fluid is in quasiequilibrium, and the density of ions relaxes very fast to the equilibrium Boltzmann distribution corresponding to the local electrostatic potential ψ, i.e., $n_\pm = e^{\mp \psi}$. This leads to the Poisson-Boltzmann equation for the electrostatic potential within the double layer satisfying the boundary condition $\psi = \psi_s$ at the surface of the motor. Furthermore, we consider the colloidal particles in which the surface potential is uniform over the surface of particle. Solving this equation gives the electrostatic potential in the inner problem; then, the Stokes equation with an electrostatic body force and no-slip boundary condition at the surface of the motor will be solved within a lubrication approximation to obtain the fluid flow profile within the double layer. The solution for the inner region provides the required boundary values for the outer region problem, i.e., the values for the potential $\psi_D(\hat{\mathbf{r}})$ at the edge of the double layer, from which the so-called zeta-potential follows as:

$$\zeta(\hat{\mathbf{r}}) = \psi_s - \psi_D(\hat{\mathbf{r}}), \tag{11}$$

and the "phoretic slip velocity," i.e., the flow velocity $\mathbf{V}_s$ at the edge of the double layer, is given by the Dukhin-Derjaguin relation[90] as

$$\mathbf{V}_s = \zeta \nabla_s \psi - 4 \ln\left(\cosh \frac{\zeta}{4}\right) \nabla_s \ln N, \tag{12}$$

where $\nabla_s = (\mathbb{I} - \hat{\mathbf{n}}\hat{\mathbf{n}}) \cdot \nabla$ denotes the derivative along the surface (to be evaluated at the edge of the Debye layer).

For the outer region, the regularity of $\nabla^2 \psi$ at the limit of $\delta \to 0$ implies that the left hand side of Eq. (3) vanishes at the same limit of negligible Debye screening length.[86] Consequently, one infers that in the outer region $(n_+ - n_-)$ is very small (of the order of δ^2 or smaller). Then, we will reach to our core approximation for the outer region: $n_+ \simeq n_-$. By applying this approximation, now we can rewrite the governing equations for the outer region. It is convenient to denote all the effective macroscale fields for the outer region by capital letters. The hydrodynamic flow is governed by the Stokes equation as

$$\nabla^2 \mathbf{V} - \nabla P + \nabla^2 \Psi \nabla \Psi = 0, \quad \nabla \cdot \mathbf{V} = 0. \tag{13}$$

The ionic densities and electrostatic potential are obtained by solving the following equations:

$$\nabla^2 N = 0, \quad \nabla \cdot (N \nabla \Psi) = 0. \tag{14}$$

The effective fields at the outer region are subjected to boundary conditions at the edge of the Debye layer ($r \approx 1$) as

$$\frac{\partial N}{\partial n} = -\dot{q}\, \hat{\mathbf{t}} \cdot \hat{\mathbf{n}}, \quad N \frac{\partial \Psi}{\partial n} = 0, \quad \Psi = \psi_s - \zeta, \quad \mathbf{V} = \mathbf{V}_s, \tag{15}$$

where $\frac{\partial}{\partial n} = \hat{\mathbf{n}} \cdot \nabla$ and $\mathbf{V}_s$ is the phoretic slip velocity given in Eq. (12). The boundary conditions at infinity read as

$$\mathbf{V}(\mathbf{r}) = -\mathbf{U} - \mathbf{\Omega} \times \mathbf{r}, \quad \nabla \Psi(\mathbf{r}) = -\epsilon\, \hat{e}. \tag{16}$$

Finally, the effective fields satisfy the same force and torque free conditions as given before in Eqs. (9) and (10).

To demonstrate how the above equations can work, consider a very simple example that corresponds to a nonactive Janus particle in the absence of electric field ($\dot{q} = \epsilon = 0$). The results can be written as

$$N_0 = 1, \quad \Psi_0(\mathbf{r}) = 0, \quad \zeta_0 = \psi_s, \quad \mathbf{U}_0 = \mathbf{\Omega}_0 = 0. \tag{17}$$

This implies that in the absence of activity and external field, the system is in the equilibrium state and the particle does not move.

V. PERTURBATIVE EXPANSION

The assumption of a thin Debye layer has simplified the governing equations, but the equations are still too difficult to be solved analytically. In order to achieve analytical solutions and to gain physical insight into the problem, we further restrict the scope of this study to the case when the surface chemical activity of the motor $\dot{q}$ and the applied electric field ϵ are small so that the activity and applied field can be treated as perturbations to the equilibrium state where the particle is not active and there is no external field. We will see later in Sec. VI that for a typical active Janus particle, the strength of the electric field and also the chemical activity belong to an interval that naturally can justify the validity of this perturbative scheme. In order to implement the perturbative expansion, we decompose the full problem of the electrophoretic active Janus particle to three distinct auxiliary problems. As defined before in Eq. (1), the first problem corresponds to the propulsive motion of an active Janus particle in the absence of external force, and we denote this problem by superscript a. The second problem that is denoted by superscript e corresponds to the electrophoresis of a passive colloidal particle. Superimposing these two problems, we will need a third contribution to recover our real problem. Denoting this contribution by symbol ae, it will collect the simultaneous effects due to both activity and electric field. Now, a perturbative expansion can be considered for the linear and angular velocities of the Janus particle as

$$\mathbf{U}^a = \sum_{m=1}^{\infty} \dot{q}^m\, \mathbf{U}_m^a, \qquad \mathbf{U}^e = \sum_{m=1}^{\infty} \epsilon^m\, \mathbf{U}_m^e,$$

$$\mathbf{U}^{ae} = \sum_{m,n=1}^{\infty} \dot{q}^m \epsilon^n \mathbf{U}_{mn}^{ae}, \quad \mathbf{\Omega}^{ae} = \sum_{m,n=1}^{\infty} \dot{q}^m \epsilon^n \mathbf{\Omega}_{mn}^{ae}.$$

Due to symmetry arguments and as is reflected in our expansion, for the first two problems of the isolated Janus motor and electrophoresis, there is no torque to change the angular orientation of the particle. We will use a similar terminology to decompose and expand all relevant fields of the problem. In Secs. V A–V C, we will present the leading order contributions to each problem defined here.

A. Isolated active particle

Here, we consider the case that an active Janus particle moves in an electrolyte solution without applying any external electric field. This problem has been considered before; for completeness, we succinctly present the calculations.[80] Applying the approximations and expansion discussed above, the governing equations up to the first order of $\dot{q}$ are simplified as follows:

$$\nabla^2 \mathbf{V}_1^a - \nabla P_1^a = 0, \quad \nabla \cdot \mathbf{V}_1^a = 0, \tag{18a}$$

$$\nabla^2 N_1^a = 0, \quad \nabla^2 \Psi_1^a = 0, \tag{18b}$$

which should be solved provided the following boundary conditions for the number density of ions and the potential on the surface of the particle:

$$\frac{\partial N_1^a}{\partial n} = -\hat{\mathbf{t}} \cdot \hat{\mathbf{n}}, \quad \frac{\partial \Psi_1^a}{\partial n} = 0, \quad \Psi_1^a = -\zeta_1^a, \quad \mathbf{r} = \hat{\mathbf{n}}. \tag{19}$$

The slip velocity has a complicated dependence on the density of ions and zeta-potential. Perturbation expansion for these variables takes a bit more calculations that are presented in Appendix A. Considering the solutions in equilibrium state, Eq. (A1) reveals that the phoretic slip velocity up to the order of $\dot{q}$ reads as

$$\mathbf{V}_{1,s}^a = \psi_s \nabla_s \Psi_1^a - 4 \ln\left(\cosh \frac{\psi_s}{4}\right) \nabla_s N_1^a, \quad \mathbf{r} = \hat{\mathbf{n}}. \tag{20}$$

At infinity, we have

$$\mathbf{V}_1^a(\mathbf{r}) = -\mathbf{U}_1^a - \Omega_1^a \times \mathbf{r}, \quad \nabla \Psi_1^a(\mathbf{r}) = 0, \quad N_1^a = 0. \tag{21}$$

Finally, the force- and torque-free conditions at the first order of $\dot{q}$ can be obtained by expanding Eqs. (9) and (10).

Solving the equations for the density and potential gives the following solutions:

$$N_1^a = \frac{1}{2r^2}(\hat{\mathbf{t}} \cdot \hat{\mathbf{r}}), \quad \Psi_1^a(\mathbf{r}) = 0, \quad \zeta_1^a = 0. \tag{22}$$

Using Eqs. (20) and (22), the slip velocity is evaluated as

$$\mathbf{V}_{1,s}^a = -2 \ln\left(\cosh \frac{\psi_s}{4}\right) \hat{\mathbf{t}} \cdot (\mathbb{I} - \hat{\mathbf{r}}\hat{\mathbf{r}}), \quad \mathbf{r} = \hat{\mathbf{n}}. \tag{23}$$

Having the slip velocity condition, we can proceed to evaluate the velocity of the particle. To this end, we employ the Lorentz reciprocal theorem in hydrodynamics which relates two solutions of the Stokes equation sharing the same geometry but with different boundary conditions.[1] By considering our main problem (moving an active particle with phoretic slip velocity) as one of the two problems and noting that this particle is force- and torque-free, the Lorentz theorem gives

$$\mathbf{U} \cdot \mathbf{F}_I + \Omega \cdot \boldsymbol{\tau}_I = -\int_{|\mathbf{r}|=1} \mathbf{V}_s \cdot \boldsymbol{\sigma}_I \cdot \hat{\mathbf{n}} \, dS, \tag{24}$$

where $\mathbf{F}_I = \int_{|\mathbf{r}|=1} \boldsymbol{\sigma}_I \cdot \hat{\mathbf{n}} \, dS$ and $\boldsymbol{\tau}_I = \int_{|\mathbf{r}|=1} (\mathbf{r} - \mathbf{r}_0) \times \boldsymbol{\sigma}_I \cdot \hat{\mathbf{n}} \, dS$ denote the force and torque exerted by the fluid on the particle in the other problem with corresponding stress tensor $\boldsymbol{\sigma}_I$, which can be chosen arbitrary. We choose a sphere moving with an arbitrary

translational or rotational velocity and no slip boundary condition on its surface as problem I and can easily see that the translational and the angular velocity of the spherical active Janus particle are given by[91]

$$\mathbf{U} = -\frac{1}{4\pi} \int_{r=1} \mathbf{V}_s \, dS, \quad \Omega = -\frac{3}{8\pi} \int_{r=1} \mathbf{r} \times \mathbf{V}_s \, dS. \tag{25}$$

Putting the slip velocity from Eq. (23) into the above equations and, then, calculating the integrals leads to the following results for translational and rotational velocities of the motor:

$$\mathbf{U}_1^a = \frac{4}{3} \ln\left(\cosh \frac{\psi_s}{4}\right)\hat{\mathbf{t}}, \quad \Omega_1^a = 0. \tag{26}$$

Following the same procedure for higher orders of $\dot{q}$ reveals that both the translational and angular velocities vanish up to the order of $\mathcal{O}(\dot{q}^3)$.

B. Electrophoresis

When the activity of the particle is neglected, the problem drops to the electrophoresis of a passive charged colloidal particle in an electrolyte solution, which is one of the well-known problems in the physics of colloidal dispersion and has been studied in different limits analytically and numerically.[81,82,92] Here, we are assuming that for this passive Janus particle, the surface electric potential is symmetric and constant over the particle. In the thin Debye layer limit and for weak electric fields, the dynamical equations for effective fields up to the first order of ϵ, i.e., $\mathbf{V}_1^e, \Psi_1^e, N_1^e$, satisfy the same equations as Eq. (18) but with different boundary conditions. The particle is passive, i.e., there is no emission/annihilation of ions on the surface of the particle. Therefore, the boundary conditions at $\mathbf{r} = \hat{\mathbf{n}}$ are given by

$$\frac{\partial N_1^e}{\partial n} = 0, \quad \frac{\partial \Psi_1^e}{\partial n} = 0, \quad \Psi_1^e = -\zeta_1^e, \quad \mathbf{r} = \hat{\mathbf{n}},$$

$$\mathbf{V}_{1,s}^e = \psi_s \nabla_s \Psi_1^e - 4 \ln\left(\cosh \frac{\psi_s}{4}\right) \nabla_s N_1^e, \quad \mathbf{r} = \hat{\mathbf{n}}, \tag{27}$$

where the slip velocity on the surface of the particle up to the order of $\mathcal{O}(\epsilon)$ is obtained according to Eq. (A1) in Appendix A. Far from the particle, the boundary conditions read

$$\mathbf{V}_1^e(\mathbf{r}) = -\mathbf{U}_1^e - \Omega_1^e \times \mathbf{r}, \quad \nabla \Psi_1^e(\mathbf{r}) = -\hat{\epsilon}, \quad N_1^e = 0, \quad r \to \infty.$$

These equations and boundary conditions result in the following solutions:

$$\Psi_1^e(\mathbf{r}) = -\left(r + \frac{1}{2r^2}\right)\hat{\epsilon} \cdot \hat{\mathbf{r}}, \quad \zeta_1^e = \frac{3}{2}\hat{\epsilon} \cdot \hat{\mathbf{r}}, \quad N_1^e(\mathbf{r}) = 0. \tag{28}$$

Then, using Eq. (27), the slip velocity is calculated as

$$\mathbf{V}_{1,s}^e = -\frac{3}{2}\psi_s \hat{\epsilon} \cdot (\mathbb{I} - \hat{\mathbf{r}}\hat{\mathbf{r}}), \quad \mathbf{r} = \hat{\mathbf{n}}. \tag{29}$$

Substituting this slip velocity in to the Lorentz equation, Eq. (25), and calculating the integrals, the velocity of the particle can be derived as follows:

$$\mathbf{U}_1^e = \psi_s \hat{\epsilon}, \quad \Omega_1^e = 0, \tag{30}$$

which describes the electrostatic velocity of a spherical colloidal particle in the Smolokowski limit.[92]

The contribution of orders $\mathcal{O}(\epsilon^2)$ and $\mathcal{O}(\epsilon^3)$ to the velocity of the particle is zero.

C. Electrophoresis of the active Janus particle

We proceed to the order of $\mathcal{O}(\dot{q}\,\epsilon)$ that both the activity and the electric field has a simultaneous contribution in the dynamics of the particle. The effective fields are given by the solutions to the following equations:

$$\nabla^2 \mathbf{V}_{11}^{ae} - \nabla P_{11}^{ae} = 0, \quad \nabla \cdot \mathbf{V}_{11}^{ae} = 0,$$
$$\nabla^2 N_{11}^{ae} = 0, \quad \nabla \cdot \left(\nabla \Psi_{11}^{ae} + N_1^a \nabla \Psi_1^e \right) = 0. \quad (31)$$

In this case, the relevant boundary conditions on the surface of the particle and at infinity read as

$$\frac{\partial N_{11}^{ae}}{\partial n} = \frac{\partial \Psi_{11}^{ae}}{\partial n} = 0, \quad \Psi_{11}^{ae} = -\zeta_{11}^{ae}, \quad \mathbf{V}_{11}^{ae} = \mathbf{V}_{11,s}^{ae}, \quad \mathbf{r} = \hat{\mathbf{n}},$$

$$\mathbf{V}_{11}^{ae}(\mathbf{r}) = -\mathbf{U}_{11}^{ae} - \Omega_{11}^{ae} \times \mathbf{r}, \quad \nabla \Psi_{11}^{ae}(\mathbf{r}) = N_{11}^{ae} = 0, \quad r \to \infty,$$

respectively, where $\mathbf{V}_{11,s}^{ae}$ is the slip velocity up to the order of $\mathcal{O}(\dot{q}\,\epsilon)$ and is taken from Eq. (A1). Solving the equation for density of ions gives $N_{11} = 0$. After inserting N_1^a and Ψ_1^e from Eqs. (22) and (28) into Eq. (31), we see that one needs to solve the following Poisson equation to achieve Ψ_{11}^{ae}:

$$\nabla^2 \Psi_{11}^{ae} = \left(\frac{1}{2r^3} + \frac{1}{4r^6} \right)(\hat{\mathbf{t}} \cdot \hat{\epsilon}) + \left(-\frac{3}{2r^3} + \frac{3}{4r^6} \right)(\hat{\epsilon} \cdot \hat{\mathbf{r}})(\hat{\mathbf{t}} \cdot \hat{\mathbf{r}}). \quad (32)$$

The solution to this equation is obtained by evaluating the following expression:[93]

$$\Psi_{11}^{ae}(\mathbf{r}) = \frac{1}{4\pi} \int \frac{\nabla^2 \Psi_{11}^{ae}}{|\mathbf{r} - \mathbf{r}'|} d\mathbf{r}' + B(\mathbf{r}), \quad (33)$$

regarding that $B(\mathbf{r})$ satisfies the Laplace equation, i.e., $\nabla^2 B(\mathbf{r}) = 0$ with a proper boundary condition given by

$$\frac{\partial B}{\partial n}\Big|_{r=1} = \frac{\partial \Phi}{\partial n}\Big|_{r=1},$$

and $\Phi(\mathbf{r}) = \frac{1}{4\pi} \int \frac{\nabla^2 \Psi_{11}^{ae}}{|\mathbf{r} - \mathbf{r}'|} d\mathbf{r}$. A direct calculation of the above integral (presented in Appendix B) reveals that Ψ_{11}^{ae} has a form as

$$\Psi_{11}^{ae}(\mathbf{r}) = \frac{1}{4}\left(\frac{1}{3r^3} - \frac{1}{r} \right)(\hat{\mathbf{t}} \cdot \hat{\epsilon}) + \frac{1}{4}\left(\frac{1}{r} - \frac{1}{r^3} + \frac{1}{2r^4} \right)(\hat{\mathbf{t}} \cdot \hat{\mathbf{r}})(\hat{\epsilon} \cdot \hat{\mathbf{r}}). \quad (34)$$

Then, by considering the boundary conditions on the surface of the particle, we can calculate the change in the zeta-potential up to $\mathcal{O}(\dot{q}\,\epsilon)$ as

$$\zeta_{11}^{ae} = -\frac{1}{6}(\hat{\mathbf{t}} \cdot \hat{\epsilon}) + \frac{1}{8}(\hat{\mathbf{t}} \cdot \hat{\mathbf{r}})(\hat{\epsilon} \cdot \hat{\mathbf{r}}). \quad (35)$$

Using the density of ions and the electric potential, we evaluate the slip velocity up to the order of $\dot{q}\,\epsilon$ as

$$\mathbf{V}_{11,s}^{ae} = \frac{1}{8}\psi_s\, \hat{\mathbf{t}} \cdot (\mathbb{I}\hat{\mathbf{r}} + \hat{\mathbf{r}}\mathbb{I} - 2\hat{\mathbf{r}}\hat{\mathbf{r}}\hat{\mathbf{r}}) \cdot \hat{\epsilon} - \frac{3}{4} \tanh \frac{\psi_s}{4} \, \hat{\mathbf{t}} \cdot (\mathbb{I}\hat{\mathbf{r}} - \hat{\mathbf{r}}\hat{\mathbf{r}}\hat{\mathbf{r}}) \cdot \hat{\epsilon}; \quad (36)$$

consequently, the translational and rotational velocities of the particle are attained by computing the integrals in Eq. (25) as

$$\mathbf{U}_{11}^{ae} = 0, \quad \Omega_{11} = \frac{3}{8} \tanh \frac{\psi_s}{4} \, \hat{\epsilon} \times \hat{\mathbf{t}}. \quad (37)$$

This contribution originates from the zeta-potential modification. One can see that up to the order of $\mathcal{O}(\dot{q}\epsilon)$, the main effect of the electric field is to rotate it along a direction parallel or antiparallel to the electric field, depending on the sign of ψ_s.

Carrying out the same procedure, we found that the perturbation terms proportional to $\mathcal{O}(\epsilon)^2$ and $\mathcal{O}(\dot{q})^2$ are zero. Details of these calculations are not included here, but we continue our calculations to find the next nonzero contributions in our perturbation analysis. The next nonzero contribution is of the order of $\mathcal{O}(\dot{q}\epsilon^2)$, which we will consider in detail in Subsection C 1.

1. Calculating $\mathbf{U}_{12}^{ae}$ and Ω_{12}^{ae}

Here, we take into consideration the second order of electric field and try to find the velocity of the motor up to the order $\mathcal{O}(\dot{q}\epsilon^2)$. To do this, the following equations should be solved:

$$\nabla^2 \mathbf{V}_{12}^{ae} - \nabla P_{12}^{ae} + \nabla^2 \Psi_{11}^{ae} \nabla \Psi_1^e = 0, \quad \nabla \cdot \mathbf{V}_{12}^{ae} = 0,$$
$$\nabla^2 N_{12}^{ae} = 0, \quad \nabla \cdot \left(\nabla \Psi_{12}^{ae} + N_1^a \nabla \Psi_{11}^{ae} \right) = 0. \quad (38)$$

These equations are subject to the boundary conditions on the surface of the motor and are given by

$$\frac{\partial N_{12}^{ae}}{\partial n} = \frac{\partial \Psi_{12}^{ae}}{\partial n} = 0, \quad \Psi_{12} = -\zeta_{12}^{ae}, \quad \mathbf{V}_{12}^{ae} = \mathbf{V}_{12,s}^{ae}, \quad \mathbf{r} = \hat{\mathbf{n}},$$

and at infinity, the conditions are given by

$$\mathbf{V}_{12}^{ae}(\mathbf{r}) = -\mathbf{U}_{12}^{ae} - \Omega_{12}^{ae} \times \mathbf{r}, \quad \nabla \Psi_{12}^{ae}(\mathbf{r}) = N_{12}^{ae} = 0, \quad r \to \infty,$$

where $\mathbf{V}_{11,s}^{ae}$ is taken from Eq. (A1). Solving these equations, we derive the results for density, electric potential, and zeta-potential as

$$N_{12}^{ae} = 0, \quad \Psi_{12}^{ae}(\mathbf{r}) = 0, \quad \zeta_{12}^{ae} = 0. \quad (39)$$

Although all fields in this order are zero, according to Eq. (A1), the slip velocity has some contributions from the lower orders and is obtained as

$$\mathbf{V}_{12,s}^{ae} = \frac{1}{4} (\hat{\mathbf{t}} \cdot \hat{\epsilon})(\mathbb{I} - \hat{\mathbf{r}}\hat{\mathbf{r}}) \cdot \hat{\epsilon} + \frac{3}{16} \hat{\mathbf{t}}(\hat{\epsilon} \cdot \hat{\mathbf{r}})^2 - \frac{9}{64}\left(1 - \tanh^2 \frac{\psi_s}{4} \right) \hat{\mathbf{t}}$$
$$\cdot (\mathbb{I} - \hat{\mathbf{r}}\hat{\mathbf{r}})(\hat{\epsilon} \cdot \hat{\mathbf{r}})^2 - \frac{3}{16} (\hat{\mathbf{t}} \cdot \hat{\mathbf{r}})(\hat{\epsilon} \cdot \hat{\mathbf{r}})^2 \hat{\mathbf{r}}. \quad (40)$$

Finally, $\mathbf{U}_{12}^{ae}$ and Ω_{12}^{ae} can be obtained by inserting the above equation into Eq. (25) and taking the integrals as

$$\mathbf{U}_{12}^{ae} = \frac{1}{960}\left(-151 + 27 \tanh^2 \frac{\psi_s}{4} \right)(\hat{\mathbf{t}} \cdot \hat{\epsilon})\hat{\epsilon} - \frac{1}{64}\left(1 + 3 \tanh^2 \frac{\psi_s}{4} \right)\hat{\mathbf{t}}, \quad (41)$$

$$\Omega^{ae}_{12} = 0.$$

In Sec. VI, we show in detail how the trajectories of active Janus particles will be modified by applying an external uniform electric field.

VI. RESULTS AND DISCUSSION

Combining all the above results, the total translational and rotational velocities of the motor up to the leading orders of perturbation analysis are given by

$$\mathbf{U} = \frac{4}{3}\ln\left(\cosh\frac{\psi_s}{4}\right)\dot{q}\,\hat{\mathbf{t}} + \psi_s\epsilon\,\hat{\boldsymbol{\epsilon}} + \frac{1}{960}\left(-151 + 27\tanh^2\frac{\psi_s}{4}\right)$$
$$\times \dot{q}\,\epsilon^2\,(\hat{\mathbf{t}}\cdot\hat{\boldsymbol{\epsilon}})\hat{\boldsymbol{\epsilon}} - \frac{1}{64}\left(1 + 3\tanh^2\frac{\psi_s}{4}\right)\dot{q}\,\epsilon^2\,\hat{\mathbf{t}}, \quad (42)$$

$$\Omega = \frac{3}{8}\tanh\frac{\psi_s}{4}\dot{q}\,\epsilon\,\hat{\boldsymbol{\epsilon}}\times\hat{\mathbf{t}}. \quad (43)$$

One should note that the above equations are written in dimensionless units. As noted before, the linear and angular speeds given by v_0 and v_0/a with $v_0 = (k_BT/e)^2(\epsilon_r/\eta a)$ can be used to recover the physical dimensions.

In typical systems of active Janus motors and electrophoresis experiments,[6,68] one has $n_\infty \sim 10^{23}$ m^{-3}, $\dot{Q} \sim 10^7$ s$^{-1}\mu$m^{-2}, $\psi_s \sim 100$ mV and $E \sim 250$ V m^{-1}, which are equivalent to dimensionless values as $\dot{q} \sim 0.1, \psi_s \sim 4.0$ and $\epsilon \sim 0.01$, regarding that at the room temperature we have $k_BT/e \sim 25$ mV. One should note that, for such a typical swimmer that is realizable in experiments, we have $\epsilon \ll 1$ and $\dot{q} \ll 1$ that justifies the validity and convergence of the perturbative expansion we have used in our analysis. Using these values, one can estimate the magnitude of the translational and the angular velocities of the motor as $U \sim 60$ μm/s and $\Omega \sim 0.2$ s^{-1}, respectively.

Interestingly, we note that, as we neglected thermal fluctuations in this study, the motion of the motor is constrained to take place in a two dimensional plane containing two vectors $\hat{\mathbf{t}}(0)$ (initial orientation of the swimmer) and $\hat{\boldsymbol{\epsilon}}$, direction of the electric field. For simplicity, we choose the x axis as the direction of the electric field $\hat{\boldsymbol{\epsilon}}$, and in this case, $\hat{\mathbf{t}}$ lies in the x–y plane such that $\cos\theta = \hat{\mathbf{t}}\cdot\hat{\boldsymbol{\epsilon}}$. In the following, we consider the case that $\dot{q} = 0.1, \epsilon = 0.01$. We start presenting results by investigating the influence of the external electric field on the speed of the motor.

First, we discuss the case of positive surface potentials, i.e., $\psi_s > 0$. From Eq. (42), one infers that applying an electric field in the direction of $\hat{\mathbf{t}}$, i.e., $\theta = 0$, causes the speed of the motor to increase with respect to the speed of an isolated motor. According to Eq. (43), this case does not induce any rotational motion for the swimmer. This increase in the speed can be understood by considering the fact that in this case both electrophoresis and activity lead the motor to move in the same direction, and thus, both effects cooperate in propelling the motor in the direction of the electric field with an enhanced speed. For the electric field applied in the direction of $-\hat{\mathbf{t}}$, i.e., $\theta = \pi$, two contributions drive the motor in opposite directions; therefore, the speed decreases with respect to the speed of the motor in the absence of the field.

On the other hand, the case of a motor with negative surface potentials is different. For $\psi_s < 0$, the speed of the motor decreases

for $\theta = 0$ and increases for $\theta = \pi$. For other initial orientations of the motor, the speed decreases due to application of the electric field to reach the same value irrespective of the sign of surface potential. Figure 2 illustrates results for two typical examples. Here, the surface potential is chosen as $\psi_s = \pm 4.0$, initial orientation is given by $\theta = \pi/3$, and other physical values are $\dot{q} = 0.1, \epsilon = 0.01$. As one can see, in both cases proceeding in time, the speed will decrease.

The most interesting impact of the electric field is its influence on orientation and direction of the Janus particle. In order to find out how the electric field affects the dynamical behavior of the motor, we follow some trajectories which start at the same position but with different initial orientations of the motor with respect to the direction of the electric field. The dynamics of the active particle is obtained by the following equations:

$$\frac{dx}{dt} = U_x, \qquad \frac{dy}{dt} = U_y, \qquad \frac{d\theta}{dt} = \Omega = \omega\sin\theta, \quad (44)$$

where all variables are dimensionless, $\omega = \frac{3}{8}\tanh\frac{\psi_s}{4}\dot{q}\,\epsilon$, and U_x, U_y, and Ω are given in Eqs. (42) and (43). The trajectory of the motor in the presence of an electric field is obtained by integrating the above equations.

For general cases, Eq. (44) can be solved numerically to give the trajectory. Some typical examples of the trajectories are illustrated in Fig. 3 for two different initial orientations $\theta_i = \pm\pi/3$ and for two different surface potentials $\psi_s = \pm 4.0$. As is reflected from Eq. (43) and also seen in Fig. 3, for any initial orientation, the electric field enforces the motor to rotate until its orientation $\hat{\mathbf{t}}$ points parallel or antiparallel to the direction of $\hat{\boldsymbol{\epsilon}}$, for cases of $\psi_s < 0$ or $\psi_s > 0$, respectively. Afterwards, the motor keeps moving toward its emitting side, i.e., in the direction of the electric field for $\psi_s < 0$ and opposite to the field for $\psi_s > 0$. This is in contrast to the electrophoresis of a passive particles, where the motion of a particle is in the direction of the electric field for positive surface potentials and against the field for negative surface potentials.

Similar behavior has been observed experimentally in Ref. 68 for dynamics of a half-coated Janus sphere composed of polystyrene and platinum moving in a solution of H_2O_2. Their results reveal
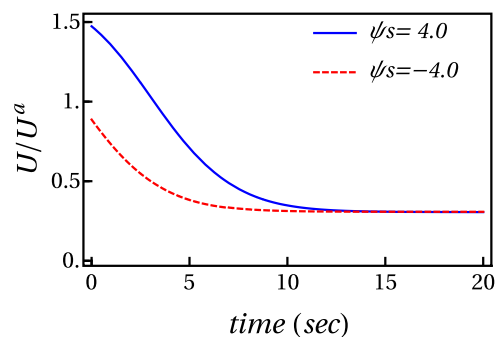
FIG. 2. The speed of the motor in the presence of an electric field normalized by its intrinsic speed U^a as a function of time. This plot corresponds to the initial configuration that $\theta = \pi/3$ for two values of surface potential and $\epsilon = 0.01$ and $\dot{q} = 0.1$.
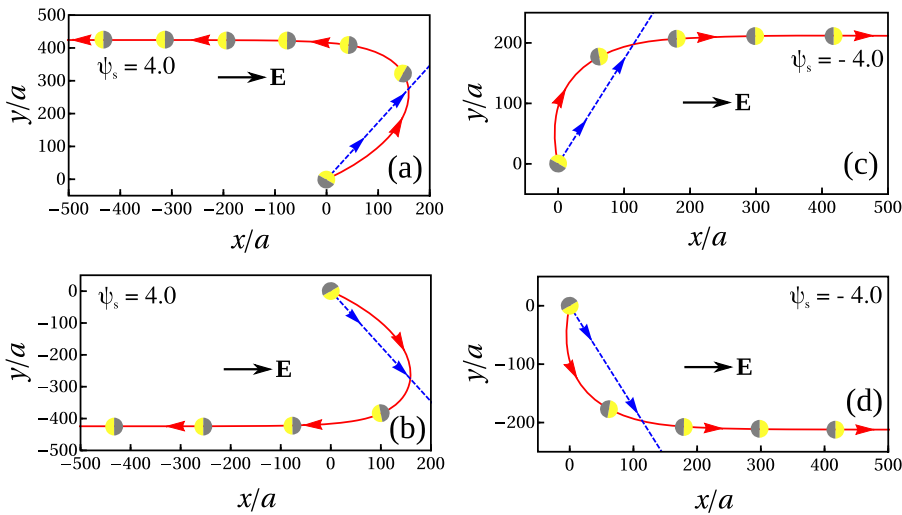
FIG. 3. Trajectories of the Janus motor in the presence of an external uniform electric field. The panels correspond to typical values $\dot{q} = 0.1, \epsilon = 0.01$ and to different surface potential [(a) and (b)] $\psi_s = 4.0$ and [(c) and (d)] $\psi_s = -4.0$ for initial orientations of the motor with respect to the direction of the electric field [(a) and (c)] $\theta_i = \pi/3$ and [(b) and (d)] $\theta_i = -\pi/3$. The dashed blue lines show the trajectory of a corresponding isolated motor, i.e., in the absence of electric field. The colored small disks indicate the motor orientation along its trajectory. The emitting side of the motor is depicted in yellow, as shown in Fig. 1.

that the surface potential is negative and then the motor reorients the polystyrene side in the direction of the applied field and moves toward its intrinsic direction of motion. One should note that in that experiment the isolated Janus particle self-propels with the polystyrene side forward.

The instantaneous orientation of the Janus particle is shown by colored disks along its trajectory in Fig. 3. As illustrated in Fig. 1, here we have shown the emitting side in yellow. In addition, the time intervals between the symbols are the same; then, the position of disks is an indication of the speed of the motor. The distance traveled by the motor between two symbols decreases during its motion, and this implies that the speed of motor decreases as time increases.

Although the angular rotation tends to orient the motor to the parallel/antiparallel direction with respect to the electric field, Eqs. (42) and (43) reveal that the time taken by the motor to reorient diverges to infinity. However, this is not physically insightful. In real situations, fluctuations with thermal or nonthermal sources do not allow us to define a precise value for the angle. We denote this unavoidable error by $\Delta\theta$; then, the final orientation of the motor is not exactly parallel/antiparallel to the field. Now, by considering $\psi_s > 0$ and integrating the equation for θ in Eq. (44), we obtain the "relaxation time" τ, the time taken by the motor to reach its final orientation $\theta_f = \pi - \Delta\theta$ from an initial orientation θ_i as follows:

$$\frac{\tau}{t_0} = \frac{1}{\omega} \ln\left(\cot\frac{\theta_i}{2} \cot\frac{\Delta\theta}{2}\right), \qquad (45)$$

where $t_0 = a/v_0 \sim 10^{-3}$ s is the time scale. For example, for the motor considered above, i.e., for values $\dot{q} = 0.1, \epsilon = 0.01, \psi_s = 4.0$ with initial orientation $\theta_i = \pi/3$ and for $\Delta\theta \sim 1° = \pi/180$ rad, the relaxation time is about 10 s. Increasing the magnitude of the electric field will decrease this time scale. This time scale is comparable with the relaxation time that is achieved in the experiment in which optical forces were used to reorient the particle.[74]

As an important remark, we investigate the stability of the final state of the particle motion. We consider the case of small

deviations from the final orientation of the particle for the case $\psi_s < 0$, i.e., $\delta\theta \ll 1$. One can do the same procedure straightforwardly for negative surface potentials. Using Eq. (42), we can write Eq. (44) as

$$\frac{d}{dt}x(t) = (a+b)\cos\delta\theta, \quad \frac{d}{dt}y(t) = a\sin\delta\theta, \quad \frac{d}{dt}\delta\theta(t) = -\omega_0\sin\delta\theta, \tag{46}$$

where $a = \frac{4}{3}\ln\left(\cosh\frac{\psi_s}{4}\right)\dot{q} - \frac{1}{64}\left(1 + 3\tanh^2\frac{\psi_s}{4}\right)\dot{q}\,\epsilon^2$, $b = \psi_s\epsilon + \frac{1}{960}\left(-151 + 27\tanh^2\frac{\psi_s}{4}\right)\dot{q}\,\epsilon^2 \, (\hat{\mathbf{t}} \cdot \hat{\boldsymbol{\epsilon}})$, and $\omega_0 = \frac{3}{8}\tanh\frac{|\psi_s|}{4}\dot{q}\,\epsilon$. For $\delta\theta \ll 1$, we have

$$\frac{d}{dt}x(t) = (a+b), \quad \frac{d}{dt}x(t) = a\delta\theta, \quad \frac{d}{dt}\theta(t) = -\omega_0\delta\theta. \tag{47}$$

For the initial state given by $x = 0$, $y = y_0$, $\delta\theta = \theta_0$, we will see that the x coordinate increases linearly with time and

$$\delta\theta \sim \theta_0 e^{-\omega_0 t}, \quad y - y_0 \sim -\frac{a\theta_0}{\omega_0}\left(e^{-\omega_0 t} - 1\right). \tag{48}$$

Therefore, at long times, the deviation from $\theta = 0$ decays and the coordinate perpendicular to the electric field, i.e., y, has a constant value $\delta y_\infty \sim \frac{a\theta_0}{\omega_0}$. This means that the final state moving along the electric field is stable against small fluctuations.

In this article, we have assumed that the surface potential over a passive Janus particle is uniform. It should be mentioned that for a passive particle, surface potential and subsequently zeta potential can have nonuniform distribution with different origins with respect to what we have considered here. This nonuniformity can originate from geometrical and electrical effects.[94] For such passive particles, dipole and quadrupole distribution of zeta potential will have extra contributions in the particle's motion. For such particles, the dipolar and quadrupolar contributions should be included to what we have presented here.

In summary, we have theoretically studied the dynamics of a self-propelled Janus particle in the field of an external force.

In our description, the strength of surface activity $\dot{q}$ and the external electric field ϵ are considered as two independent parameters, and it is shown that the resulted trajectory of the Janus particle is very sensitive to these parameters. We have shown, by tuning the electric field and the surface activity, that it is possible to control the dynamics of the particle and operate it in a desired manner.

Finally, it should be mentioned that for realistic experimental situations, interaction with confining boundaries is unavoidable. To have a complete control on the trajectory of an active Janus particle, the effects of walls should be considered carefully.

ACKNOWLEDGMENTS

APPENDIX A: EXPANSION OF V_s IN TERMS OF $\dot{q}$ AND ϵ

Here, we present the expansion of the phoretic slip velocity,

$$\mathbf{V}_s = \zeta \nabla_s \Psi - 4 \ln\left(\cosh \frac{\zeta}{4}\right) \nabla_s N,$$

in terms of $\dot{q}$ and ϵ as follows:

$$
\begin{aligned}
\mathbf{V}_s \approx\ & \zeta_0 \nabla_S \Psi_0 - 4z_0 \nabla_s N_0 \\
& + \dot{q}\left(\zeta_0 \nabla_S \Psi_1^a + \zeta_1^a \nabla_S \Psi_0 - 4z_0 \nabla_s N_1^a - \zeta_1^a \tanh \frac{\zeta_0}{4} \nabla_s N_0 \right) \\
& + \epsilon\left(\zeta_0 \nabla_S \Psi_1^e + \zeta_1^e \nabla_S \Psi_0 - 4z_0 \nabla_s N_1^e - \zeta_1^e \tanh \frac{\zeta_0}{4} \nabla_s N_0 \right) \\
& + \dot{q}\epsilon\bigg(\zeta_0 \nabla_S \Psi_{11}^{ae} + \zeta_{11}^{ae} \nabla_S \Psi_0 - 4z_0 \nabla_s N_{11}^{ae} \\
& \quad - \zeta_{11}^{ae} \tanh \frac{\zeta_0}{4} \nabla_s N_0 - \frac{1}{4}\zeta_1^a \zeta_1^e \operatorname{sech}^2 \frac{\zeta_0}{4} \nabla_s N_0 \bigg) \\
& + \dot{q}\epsilon^2\bigg(\zeta_0 \nabla_S \Psi_{12}^{ae} + \zeta_{12}^{ae} \nabla_S \Psi_0 - 4z_0 \nabla_s N_{12}^{ae} \\
& \quad - \left(\zeta_{12}^{ae} - \frac{3}{32}\zeta_1^a \zeta_1^{e\,2}\right) \tanh \frac{\zeta_0}{4} \nabla_s N_0 \\
& \quad - \frac{1}{4}(\zeta_1^a \zeta_2^e + \zeta_1^e \zeta_{11}^{ae}) \operatorname{sech}^2 \frac{\zeta_0}{4} \nabla_s N_0 \bigg),
\end{aligned}
\tag{A1}
$$

where $z_0 = \ln(\cosh(\zeta_0/4))$ and we keep only the terms that lead to nonzero velocity. Higher orders can be evaluated straightforwardly.

APPENDIX B: CALCULATING Ψ_{11}^{ae}

In this appendix, we calculate Ψ_{11}^{ae}, where

$$\Psi_{11}^{ae} = \Phi(\mathbf{r}) + F(\mathbf{r}), \quad \nabla^2 F(\mathbf{r}) = 0, \quad \frac{\partial F(\mathbf{r})}{\partial r}\Big|_{r=1} = -\frac{\partial \Phi(\mathbf{r})}{\partial r}\Big|_{r=1},$$

and

$$\Phi(\mathbf{r}) = \frac{1}{4\pi} \int \frac{\nabla N_1^a(\mathbf{r}') \cdot \nabla \Psi_1^e(\mathbf{r}')}{|\mathbf{r} - \mathbf{r}'|} d\mathbf{r},$$

where $F(\mathbf{r})$ is introduced in order to satisfy the boundary condition on the surface of the motor, i.e., $\frac{\partial \Psi_{11}^{ae}}{\partial r}\big|_{r=1} = 0$ should be achieved. By

plugging Eqs. (22) and (28) into the above equation, and expanding $1/|\mathbf{r} - \mathbf{r}'|$, $\hat{\mathbf{r}}$, and $\hat{\mathbf{r}}'$ in terms of spherical harmonics $Y_{nm}(\theta, \phi)$,[95] one obtains Φ as follows:

$$\Phi(\mathbf{r}) = \epsilon\,\dot{q}\,(\hat{\epsilon}\cdot\hat{\mathbf{t}})\left(\frac{1}{10r^3} - \frac{1}{4r}\right) + \frac{1}{5}\epsilon\,\dot{q}\,(\hat{\mathbf{t}}\cdot\hat{\mathbf{r}})(\hat{\epsilon}\cdot\hat{\mathbf{r}})\left(\frac{5}{8r^4} + \frac{5}{4r} - \frac{3}{2r^3}\right).$$
(B1)

Then, the boundary condition of $F(\mathbf{r})$ on the surface of the motors is evaluated as

$$\frac{\partial F(\mathbf{r})}{\partial r}\Big|_{r=1} = \frac{1}{20}(\hat{\epsilon}\cdot\hat{\mathbf{t}}) - \frac{3}{20}(\hat{\mathbf{t}}\cdot\hat{\mathbf{r}})(\hat{\epsilon}\cdot\hat{\mathbf{r}}).$$

Solving $\nabla^2 F(\mathbf{r}) = 0$ using the spherical harmonics and employing the above condition, one arrives at

$$F(\mathbf{r}) = -\frac{1}{60r^3}\,\hat{\mathbf{t}}\cdot(\mathbf{I} - 3\hat{\mathbf{r}}\hat{\mathbf{r}})\cdot\hat{\epsilon}.$$
(B2)

Therefore, Ψ_{11}^{ae} is obtained as

$$\Psi_{11}^{ae} = \epsilon\,\dot{q}\,(\hat{\epsilon}\cdot\hat{\mathbf{t}})\left(\frac{1}{12r^3} - \frac{1}{4r}\right) + \epsilon\,\dot{q}\,(\hat{\mathbf{t}}\cdot\hat{\mathbf{r}})(\hat{\epsilon}\cdot\hat{\mathbf{r}})\left(\frac{1}{8r^4} + \frac{1}{4r} - \frac{1}{4r^3}\right).$$
(B3)

REFERENCES

[1] J. Happel and H. Brenner, *Low Reynolds Number Hydrodynamics: With Special Applications to Particulate Media* (Martinus Nijhoff, Hague, The Netherlands, 2012).

[2] E. M. Purcell, Am. J. Phys. **45**, 3 (1977).

[3] E. Lauga, Soft Matter **7**, 3060 (2011).

[4] A. Walther and A. H. E. Müller, Soft Matter **4**, 663 (2008).

[5] A. Walther and A. H. E. Müller, Chem. Rev. **113**, 5194 (2013).

[6] W. F. Paxton, K. C. Kistler, C. C. Olmeda, A. Sen, S. K. Angelo, Y. Cao, T. E. Mallouk, P. E. Lammert, and V. H. Crespi, J. Am. Chem. Soc. **126**, 13424 (2004).

[7] S. Sundararajan, P. E. Lammert, A. W. Zudans, V. H. Crespi, and A. Sen, Nano Lett. **8**, 1271 (2008).

[8] L. Baraban, D. Makarov, R. Streubel, I. Monch, D. Grimm, S. Sánchez, and O. G. Schmidt, ACS Nano **6**, 3383 (2012).

[9] W. Gao, D. Kagan, O. Pak, C. Clawson, S. Campuzano, E. Chuluun-Erdene, E. Shipton, E. E. Fullerton, L. Zhang, E. Lauga, and J. Wang, Small **8**, 460 (2012).

[10] Y. Yoshizumi, T. Honegger, K. Berton, H. Suzuki, and D. Peyrade, Small **11**, 5630 (2015).

[11] J. Guo, J. J. Gallegos, A. R. Tom, and D. Fan, ACS Nano **12**, 1179 (2018).

[12] P. Sundararajan, J. Wang, L. A. Rosen, A. Procopio, and K. Rosenberg, Chem. Eng. Sci. **178**, 199 (2018).

[13] D. Patra, S. Sengupta, W. Duan, H. Zhang, R. Pavlick, and A. Sen, Nanoscale **5**, 1273 (2013).

[14] D. Kagan, R. Laocharoensuk, M. Zimmerman, C. Clawson, S. Balasubramanian, D. Kang, D. Bishop, S. Sattayasamitsathit, L. Zhang, and J. Wang, Small **6**, 2741 (2010).

[15] F. Mou, C. Chen, Q. Zhong, Y. Yin, H. Ma, and J. Guan, ACS Appl. Mater. Interfaces **6**, 9897 (2014).

[16] Y. Wu, X. Lin, Z. Wu, H. Möhwald, and Q. He, ACS Appl. Mater. Interfaces **6**, 10476 (2014).

[17] K. U. Cheang, K. Lee, A. A. Julius, and M. J. Kim, Appl. Phys. Lett. **105**, 083705 (2014).

[18] J. Li, B. E. de Ávila, W. Gao, L. Zhang, and J. Wang, Sci. Rob. **2**, eaam6431 (2017).

[19] Y. Gao and Y. Yu, J. Am. Chem. Soc. **135**, 19091 (2013).

[20] W. Wang, S. Li, L. Mair, S. Ahmed, T. J. Huang, and T. E. Mallouk, Angew. Chem., Int. Ed. **53**, 3201 (2014).

[21]W. Gao, R. Dong, S. Thamphiwatana, J. Li, W. Gao, L. Zhang, and J. Wang, ACS Nano **9**, 117 (2015).

[22]J. Shao, M. Abdelghani, G. Shen, S. Cao, D. S. Williams, and J. C. van Hest, ACS Nano **12**, 4877 (2018).

[23]J. Li, O. E. Shklyaev, T. Li, W. Liu, H. Shum, I. Rozen, A. C. Balazs, and J. Wang, Nano Lett. **15**, 7077 (2015).

[24]Q. Zhang, L. Liu, C. Pan, and D. Li, J. Mater. Sci. **53**, 27 (2018).

[25]J. Li, W. Gao, R. Dong, A. Pei, S. Sattayasamitsathit, and J. Wang, Nat. Commun. **5**, 5026 (2014).

[26]B. Jurado-Sánchez, S. Sattayasamitsathit, W. Gao, L. Santos, Y. Fedorak, V. V. Singh, J. Orozco, M. Galarnyk, and J. Wang, Small **11**, 499 (2015).

[27]N. Ali, B. Zhang, H. Zhang, W. Li, W. Zaman, L. Tian, and Q. Zhang, Fuel **141**, 258 (2015).

[28]L. Soler, V. Magdanz, V. M. Fomin, S. Sánchez, and O. G. Schmidt, ACS Nano **7**, 9611 (2013).

[29]D. Vilela, J. Parmar, Y. Zeng, Y. Zhao, and S. Sánchez, Nano Lett. **16**, 2860 (2016).

[30]Q. Zhang, R. Dong, Y. Wu, W. Gao, Z. He, and B. Ren, ACS Appl. Mater. Interfaces **9**, 4674 (2017).

[31]D. Vilela, M. M. Stanton, J. Parmar, and S. Sánchez, ACS Appl. Mater. Interfaces **9**, 22093 (2017).

[32]S. Wang, Z. Jiang, S. Ouyang, Z. Dai, and T. Wang, ACS Appl. Mater. Interfaces **9**, 23974 (2017).

[33]J. A. Delezuk, D. E. Ramírez-Herrera, B. E. F. de Ávila, and J. Wang, Nanoscale **9**, 2195 (2017).

[34]B. Jurado-Sánchez, M. Pacheco, J. Rojo, and A. Escarpa, Angew. Chem., Int. Ed. **129**, 7061 (2017).

[35]D. Kagan, P. Calvo-Marzal, S. Balasubramanian, S. Sattayasamitsathit, K. M. Manesh, G. Flechsig, and J. Wang, J. Am. Chem. Soc. **131**, 12082 (2009).

[36]Y. Yi, L. Sanchez, Y. Gao, and Y. Yu, Analyst **141**, 3526 (2016).

[37]T. R. Kline, W. F. Paxton, T. E. Mallouk, and A. Sen, Angew. Chem., Int. Ed. **117**, 754 (2005).

[38]J. R. Howse, R. A. L. Jones, A. J. Ryan, T. Gough, R. Vafabakhsh, and R. Golestanian, Phys. Rev. Lett. **99**, 048102 (2007).

[39]I. Buttinoni, G. Volpe, F. Kümmel, G. Volpe, and C. Bechinger, J. Phys.: Condens. Matter **24**, 284129 (2012).

[40]J. M. Catchmark, S. Subramanian, and A. Sen, Small **1**, 202 (2005).

[41]L. Qin, M. J. Banholzer, X. Xu, L. Huang, and C. A. Mirkin, J. Am. Chem. Soc. **129**, 14870 (2007).

[42]J. L. Moran, P. M. Wheat, and J. D. Posner, Phys. Rev. E **81**, 065302(R) (2010).

[43]M. N. Popescu, S. Dietrich, M. Tasinkevych, and J. Ralston, Eur. Phys. J. E **31**, 351 (2010).

[44]S. J. Ebbens and J. R. Howse, Langmuir **27**, 12293 (2011).

[45]R. Golestanian, T. B. Liverpool, and A. Ajdari, New J. Phys. **9**, 126 (2007).

[46]J. L. Moran and J. D. Posner, J. Fluid Mech. **680**, 31 (2011).

[47]S. Michelin and E. Lauga, J. Fluid Mech. **747**, 572 (2014).

[48]B. Sabass and U. Seifert, J. Chem. Phys. **136**, 064508 (2012).

[49]N. Sharifi-Mood, J. Koplik, and C. Maldarelli, Phys. Fluids **25**, 012001 (2013).

[50]J. L. Moran and J. D. Posner, Annu. Rev. Fluid Mech. **49**, 511 (2017).

[51]J. Katuri, X. Ma, M. M. Stanton, and S. Sánchez, Acc. Chem. Res. **50**, 2 (2016).

[52]L. C. Bradley, K. J. Stebe, and D. Lee, J. Am. Chem. Soc. **138**, 11437 (2016).

[53]S. Michelin and E. Lauga, Sci. Rep. **7**, 42264 (2017).

[54]R. Dong, Y. Hu, Y. Wu, W. Gao, B. Ren, Q. Wang, and Y. Cai, J. Am. Chem. Soc. **139**, 1722 (2017).

[55]D. Zhou, Y. C. Li, P. Xu, N. S. McCool, L. Li, W. Wang, and T. E. Mallouk, Nanoscale **9**, 75 (2017).

[56]S. Palagi and P. Fischer, Nat. Rev. Mater. **3**, 113 (2018).

[57]G. Volpe, I. Buttinoni, D. Vogt, H. Kümmerer, and C. Bechinger, Soft Matter **7**, 8810 (2011).

[58]A. A. Solovev, S. Sánchez, and O. G. Schmidt, Nanoscale **5**, 1284 (2013).

[59]A. Zöttl and H. Stark, Phys. Rev. Lett. **112**, 118101 (2014).

[60]H. Masoud and M. J. Shelley, Phys. Rev. Lett. **112**, 128304 (2014).

[61]C. Bechinger, R. Di Leonardo, H. Löwen, C. Reichhardt, G. Volpe, and G. Volpe, Rev. Mod. Phys. **88**, 045006 (2016).

[62]R. Di Leonardo, Nat. Mater. **15**, 1057 (2016).

[63]D. G. Crowdy, J. Fluid Mech. **735**, 473 (2013).

[64]W. E. Uspal, M. N. Popescu, S. Dietrich, and M. Tasinkevych, Soft Matter **11**, 434 (2015).

[65]W. E. Uspal, M. N. Popescu, S. Dietrich, and M. Tasinkevych, Phys. Rev. Lett. **117**, 048002 (2016).

[66]A. Zöttl and H. Stark, J. Phys.: Condens. Matter **28**, 253001 (2016).

[67]J. Simmchen, J. Katuri, W. E Uspal, M. N. Popescu, M. Tasinkevych, and S. Sánchez, Nat. Commun. **7**, 10598 (2016).

[68]S. Das, A. Garg, A. I. Campbell, J. R. Howse, A. Sen, D. Velegol, R. Golestanian, and S. Ebbens, Nat. Commun. **6**, 8999 (2015).

[69]C. Liu, C. Zhou, W. Wang, and H. P. Zhang, Phys. Rev. Lett. **117**, 198001 (2016).

[70]S. Palagi, A. G. Mark, S. Y. Reigh, K. Melde, T. Qiu, H. Zeng, C. Parmeggiani, D. S. Martella, A. Sanchez-Castillo, N. Kapernaum, F. Giesselmann, D. Wiersma, E. Lauga, and P. Fischer, Nat. Mater. **15**, 647 (2016).

[71]E. F. Semeraro, R. Dattani, and T. Narayanan, J. Chem. Phys. **148**, 014904 (2018).

[72]C. Lozano, J. R. Gomez-Solano, and C. Bechinger, New J. Phys. **20**, 015008 (2018).

[73]A. Demirors, M. T. Akan, E. Poloni, and A. R. Studart, Soft Matter **14**, 4741 (2018).

[74]C. Lozano, B. ten Hagen, H. Löwen, and C. Bechinger, Nat. Commun. **7**, 12828 (2016).

[75]W. Li, X. Wu, H. Qin, Z. Zhao, and H. Liu, Adv. Funct. Mater. **26**, 3164 (2016).

[76]S. Thakur, J. X. Chen, and R. Kapral, Angew. Chem., Int. Ed. **50**, 10165 (2011).

[77]T. Bickel, G. Zecua, and A. Würger, Phys. Rev. E **89**, 050303(R) (2014).

[78]A. Geiseler, P. Hänggi, and F. Marchesoni, Sci. Rep. **7**, 41884 (2017).

[79]T. Xu, F. Soto, W. Gao, R. Dong, V. Garcia-Gradilla, E. Maganna, X. Zhang, and J. Wang, J. Am. Chem. Soc. **137**, 2163 (2015).

[80]P. Bayati and A. Najafi, J. Chem. Phys. **144**, 134901 (2016).

[81]W. B. Russel, D. A. Saville, and W. R. Schowalter, *Colloidal Dispersions* (University Press, Cambridge, UK, 1989).

[82]H. Ohshima, *Theory of Colloid and Interfacial Electric Phenomena* (Academic Press, London, UK, 2006).

[83]A. T. Brown, W. C. K. Poon, C. Holm, and J. de Graaf, Soft Matter **13**, 1200 (2017).

[84]P. Bayati, M. N. Popescu, W. E. Uspal, S. Dietrich, and A. Najafi (unpublished).

[85]J. F. Brady, J. Fluid Mech. **667**, 216 (2011).

[86]E. Yariv, Proc. R. Soc. A **467**, 1645 (2011).

[87]O. Schnitzer and E. Yariv, J. Fluids **27**, 031701 (2015).

[88]E. Yariv, J. Fluid Mech. **655**, 105 (2010).

[89]Y. Ben and H. C. Chang, J. Fluid Mech. **461**, 229 (2002).

[90]D. C. Prieve, J. L. Anderson, J. P. Ebel, and M. E. Lowell, J. Fluid Mech. **148**, 247 (1984).

[91]S. Saha, R. Golestanian, and S. Ramaswamy, Phys. Rev. E **89**, 062316 (2014).

[92]R. W. O'Brien and L. R. White, J. Chem. Soc. Faraday **74**, 1607 (1978).

[93]J. D. Jackson, *Classical Electrodynamics* (Wiley, 1999).

[94]M. C. Fair and J. L. Anderson, J. Colloid Interface Sci. **127**, 388 (1989).

[95]G. B. Arfken, H. J. Weber, and F. E. Harris, *Mathematical Methods for Physicists: A Comprehensive Guide* (Academic Press, Oxford, UK, 2011).